# The importance of impoundment ecosystems to global organic carbon cycling and climate change : Falls Lakes, NC

## Key questions this research addresses

1) How do total suspended matter (TSM) concentrations vary during an annual period and what is the relationship between TSM, particulate organic concentrations (POC) and water discharge rates. (Objective 1)

2) How have the sediment and carbon accumulation rates changed over the lifetime of the reservoir? (Objective 2)

3) What are the main sources of the organic carbon accumulated in Falls Lake bottom sediments? (Objective 3)

**Narrative: Findings**

## Objective 1

Particulate materials play a dominant role in the transport of vital elements in river systems. A large fraction of riverine flux is in particulate form (Phosphorus~ 85%, Nitrogen ~40-85%, Organic Carbon ~ 65% *(Meybeck, 1982; Seitzinger et al., 2005, Mayer et al., 1998 and Seitzinger et al., 2005)*. Prior to this study, very little has been documented regarding sediment input into Falls Lake. The four major inputs (Flat River, Eno River, Little River and Ellerbe Creek) make up approximately 70% of the freshwater input to Falls Lake. However, no rating curves have been constructed as a means to predict suspended sediment concentration loads as a function of water discharge, a parameter which is readily available daily via USGS reporting stations online. The first major objective of this study was to examine sediment rating curves that may enable us to predict total suspended matter (TSM) concentrations based on water discharge in Cubic Feet per Second (CFS), which is readily available from the US Geological Survey. With the exception of Figures 1- 4 of this report, water discharge will be expressed in units of Cubic Meters per Second (CMS) rather than than CFS units used by the US Geological Survey. A unit conversion of CMS = CFS/ 35.314 is used.

Objective 1 of this study was to examine sediment rating curves that may enable us to predict total suspended matter (TSM) concentrations based on water discharge (in CFS) which is readily available online at https://m.waterdata.usgs.gov/ from the US Geological Survey. The ranges in discharge values were small for Ellerbe Creek (15 - 150 CFS) and Little River (5 - 85 CFS) and therefore we collected no samples that represent medium to high discharge stages (Appendix Figure 1and 4, respectively). For this reason the TSM vs Discharge relationship for these two sites is best represented by linear regressions with $R^2$ values of 0.96 and 0.94 respectively (Fig. 1 and Appendic Fig. 4 respectively). Discharge for Eno River (Appendix Fig. 2), Flat River (Appendix Fig.3), and Little River (Appendix Fig. 4) remained steady and relatively low throughout all sampling dates except for the 14 December 2019 date. The Flat River had an additional high discharge during the 2/17 /20 sampling period.

Typical rating curves that represent the full range in annual discharge are logarithmic relationships with an initial steep increase in TSM at lower discharge values; reaching an asymptote in TSM values as discharge reaches maximum values. The range in discharge for the Eno and Flat Rivers were wide enough to observe a portion of the asymptote at 50 mg/l TSM for the Eno ($R^2 = 0.85$) and 70 mg/l TSM for the Flat ($R^2 = 0.88$) (Figure 2. and Appendix Figure 5, respectively). In all four river/creek inputs, good rating curves were established to adequately predict TSM values at a given location and discharge. The weakness of the current rating curves is the uncertainty in predicted values when discharge exceed the values that we sampled in this study.

### Relationship between Suspended Sediment Concentration and Water Discharge

The ranges in discharge values were large for all four locations. The TSM vs Discharge relationship for Ellerbe Creek (Fig. 2) and Little River (Appendix Fig. 6) is best represented by linear regressions with $R^2$ values of 0.98 and 0.95 respectively. A linear relationship indicates that discharge rarely results in water levels that are high up on the banks (where the slope increases) or levels that overbank.

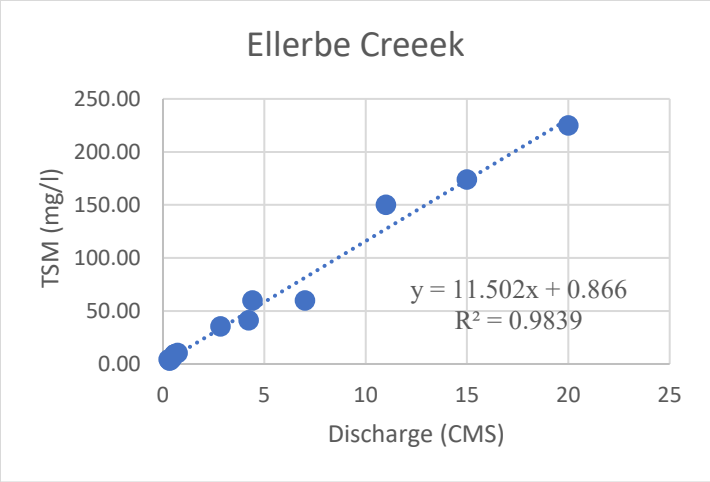


**Figure 1** shows the relationship between water discharge (CMS cubic meters per second) and TSM (total suspended matter; mg/l) for Ellerbe Creek

Eno River (Fig. 2) and Flat River (Appendix Fig. 5) display a more typical rating curves that represent the full range in annual discharge are logarithmic relationship with an initial steep increase in TSM at lower discharge values; reaching an asymptote in TSM values as discharge reaches maximum values. The range in discharge for the Eno (Fig. 2) and Flat Rivers (Appendix Fig 5) asymptote at 50 mg/l TSM for the Eno ($R^2 = 0.85$) and 60 mg/l TSM for the Flat ($R^2 = 0.88$).

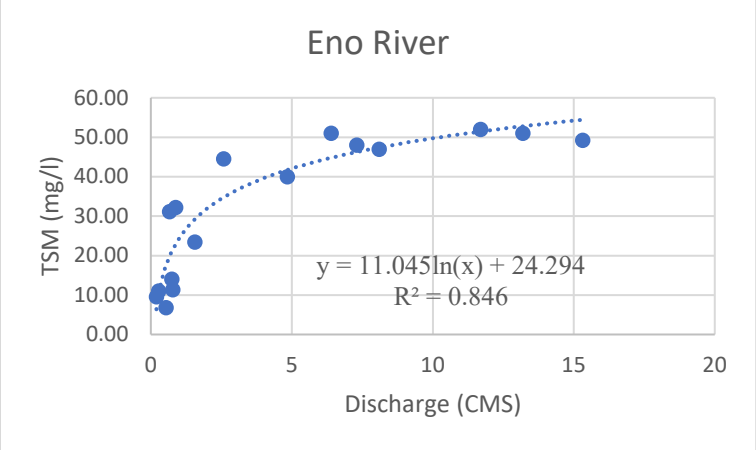


**Figure 2** shows the relationship between water discharge (CMS cubic meters per second) and TSM (total suspended matter; mg/l) for Eno River

In all four river/creek inputs good rating curves were established to adequately predict TSM values at a given location and discharge. The weakness of the current rating curves is the uncertainty in predicted values when discharge exceed the values that we sampled in this study.

**POC as a function of TSM**

Particulate Organic Carbon (POC) values in ug/l appear to be strongly correlated with TSM values (mg/l). Therefore it is possible to predict POC values of Falls Lake inputs based on discharge values. This is illustrated in Figure 4 for Ellerbe Creek ($R^2 = 0.90$), and Figure 5 for Eno River ($R^2 = 0.88$). Appendix figure 6 and 7 illustrate the carbon vs discharge curves for the Little and Flat Rivers, respectively.

Maximum POC values observed were approximately 5500, 14,500, 4500 and 7500 ug/l for Ellerbe Creek, Eno, Flat and Little Rivers, respectively (Fig. 3, 4, Appendix Fig. 6 and 7 , respectively). POC to TSM correlations are best represented by a logarithmic relationship with $R^2$ values of 0.91, 0.89, 0.81 and 0.91 for Ellerbe Creek, Eno, Flat and Little Rivers, respectively. As long as TSM values are in the range of 0-70 mg/l (as we observed) the POC:TSM curve that we have constructed will do a very good job of predicting POC values of suspended matter entering Falls Lake.

The results of this study demonstrate that total suspended matter (TSM) can be predicted (with an $R^2$ of 0.85 or better) using water discharge data readily available online from the USGS. In a similar manner, particulate carbon concentrations can be predicted (with an $R^2$ of 0.81 or better) using USGS water discharge values. This should be of great value to watershed modelers to help tune their models.

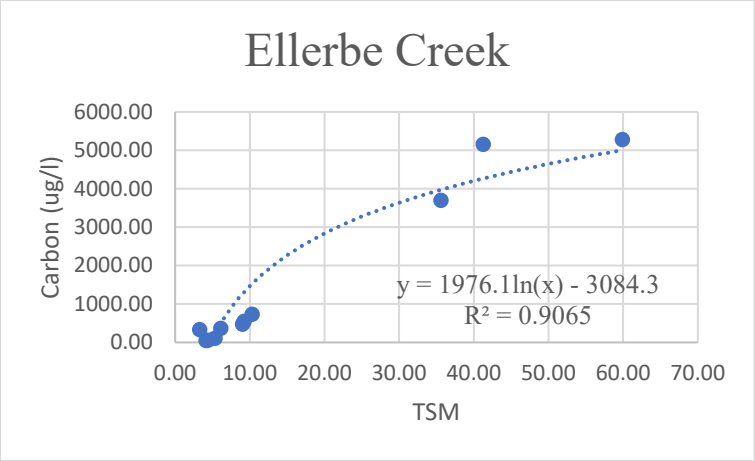


**Figure 3** Shows the relationship between TSM and carbon (ug/L) for Ellerbe Creek.

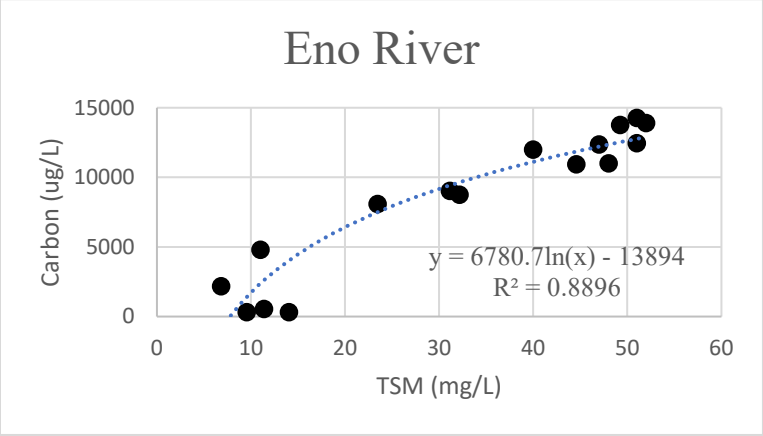


**Figure 4.** Relationship between particulate carbon concentrations in ug/l and total suspended matter concentrations (TSM) in mg/l for the Eno River

**Percent Carbon as a function of TSM**

Percent Carbon content for suspended sediments provide a semi-quantitiative approach to identifing sources of organic matter in each of the river/creek inputs. There are many other more quantitative tracers that can be used to better identify the types of soils and vegetation from which suspended sediment originate (e.g., stable isotopes of C, N; See Objective 3) but %C and C:N ratios are useful for first insights without the high expense of those alternative approaches. For Ellerbe Creek, Eno, Flat and Little Rivers, the range in %C values throughout the sampling period are well constrained (2-10, 2-5, 5-20 and 8-12,

respectively) Appendix Figures 8, 9, 10, and 11). In general an inverse relationship between %C and suspended sediment grain size is observed in world rivers. The correlation between %C and TSM is poor for all four river/creeks ($R^2$ ranging from 0.004 to 0.37) while the %C values remain relatively constant across the entire TSM range indicates that the sediment being supplied in each of the four basins are similar in character (Appendic Figures 8 - 11).

The correlation between TSM and %C is poor for all four rivers/creek. $R^2$ values range from 0.004 to 0.33 (Appendix Figures 8–11). These poor correlations are most likely due to variability in the carbon composition and grain size between each suspended sediment sample. Studies of %C in global rivers have noted that high %C samples have a higher organic carbon content than low %C samples.

**C:N ratios as an indicator of Carbon sources within the drainage basins**

The C:N ratio of particulate samples is an indicator of the source of the particulates in the system. Ellerbe Creek (Fig. 5) has the largest range in C:N values which indicates that Ellerbe Creek has the largest range of organic carbon sources during the year. C:N molar ratios of suspended sediments can provide insights as to the source of the organic matter in each sample collected. Figure 6 illustrates some possible sources within the watersheds of Falls Lake. Given the range in C:N observed during this study, a combination of sources are suggested for each river/creek. The correlation between C:N ratio and TSM is poor for Eno, Flat and Little Rivers (Appendix Fig. 12 - 14) indicating that the organic carbon is similar within these watersheds. With the exception of Ellerbe Creek the most likely sources of organic matter discharged into Falls Lake come from soil organic matter. A more sophisticated used of source tracers are used under Objective 3 to test these conclusions. Ellerbe Creek, which has a large proportion of urban environments within its watershed, has lower C:N values which indicate the influence of human inputs such as fertilizer, septic, sewage.

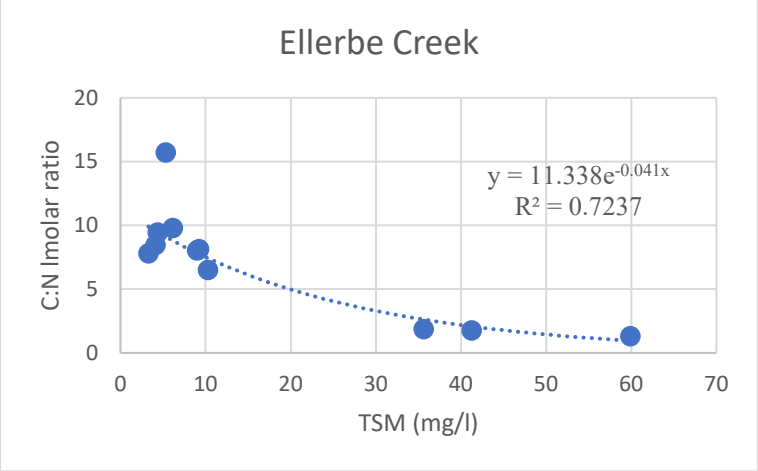


**Figure 5.** Shows the relationship between the C:N ratio and discharge for Ellerbe Creek. Mean values is 7.16

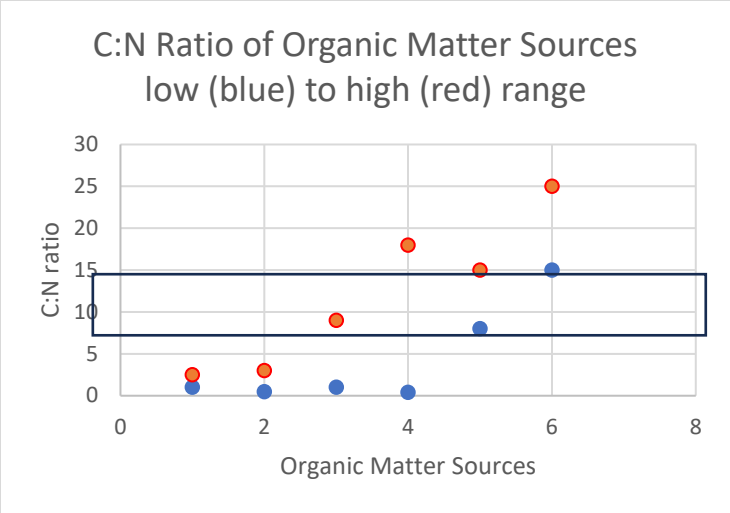


*1 Septic, 2 Sewage, 3 Forest, 4 Fertilizwer, 5 Soil organic matter, 6 Terrestrial plants*

| **Site** | **C:N Range** | **Possible Sources** |
|---|---|---|
| Ellerbe Creek | 2-16 | fertilizer, septic, sewage |
| Eno | 8-14 | soil organic matter, fertilizer |
| Flat | 8-12 | soil organic matter, fertilizer |
| Little | 7-11 | soil organic matter, fertilizer |

**Figure 6** Shows the C:N range for each site and representative ranges for 6 potential organic matter sources. Given the ovserved ranges for C:N, possible sources of organic matter is suspended sediments collected are suggested.

## Objective 2

Based on sediment thickness there was a general impression that sediment deposition rates are higher in the upper lake than in the lower lake. However, no quantitative measures of sedimentation rates existed before this study. Seasonal deposition in Falls Lake is likely to vary based on seasonal factors such as water discharge rates and interannual factors such as flood/drought conditions in the drainage basin. Both seasonal deposition rates and decadal sediment accumulations rates provide critical information needed to evaluate the flux of particle associated materials such as carbon, nutrients (N and P) and contaminants

Falls Lake covers an area of 50.2 $km^2$, which is dominantly the floodplain of the Neuse River before it was flooded (Appendix Table 1 and Fig. 7). Eighty percent (80%) of the discharge entering Falls Lake comes from five rivers and streams in the upper region of the reservoir. In the proximal half of the lake, the reservoir covers a relatively wide floodplain. This is greatly contrasted by the distal half of the reservoir towards the dam, which is significantly narrower, more channelized, and deeper on average. The watershed of Falls Lake covers 2,000 $km^2$ of land including approximately 200,000 people. This region is impacted greatly by development. The watershed includes Raleigh and Durham - significant parts of one of the fastest growing metro areas in the United States. The population of this region is predicted to increase by 50% from 2019 to 2025, and development of the watershed will continue to grow to meet this demand. As of 2019, 72.6% of land coverage in the basin is forest, 16.8% is farmland and pastureland and 7.3% is urban. Continued growth is a constant threat to the forest coverage in the region. (Deamer, 2009).

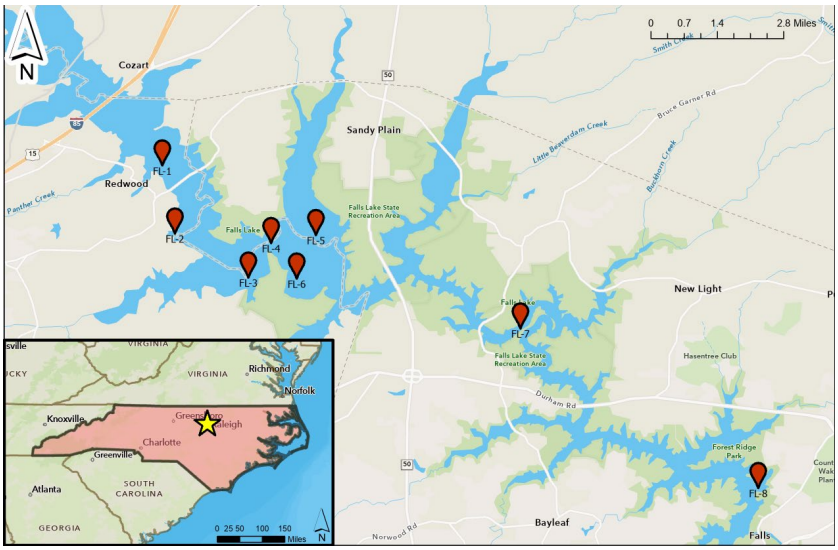

Figure 7. Locations for cores collected

*$^{210}$Pb Profiles*

Total $^{210}$Pb profiles for each core, plotted against depth, are shown in Figure 8. All cores, except for FL2 and 3, reached background levels of supported $^{210}$Pb within the core collected and $^{210}Pb_{xs}$ values were calculated as total $^{210}$Pb minus background. The missing $^{210}$Pb inventories and $^{210}Pb_{xs}$ values for FL2 and 3 were calculated based on methods outlined in Appleby (1998). Excess $^{210}$Pb inventories (dpm cm$^{-2}$) for each 1 cm layer is the product of $C_x * DBD_x * X$, where $C_x$ is the $^{210}Pb_{xs}$ activity, $DBD_x$ is the dry bulk density and X is the layer thickness. Surface $^{210}Pb_{xs}$ activities for cores FL1- 4 are similar at ~4 dpm g$^{-1}$, values for FL5 and 6 are much lower (~2 dpm g$^{-1}$), and surface $^{210}Pb_{xs}$ activities for distal sites (FL7 and 8) are highest (~10 dpm g$^{-1}$).

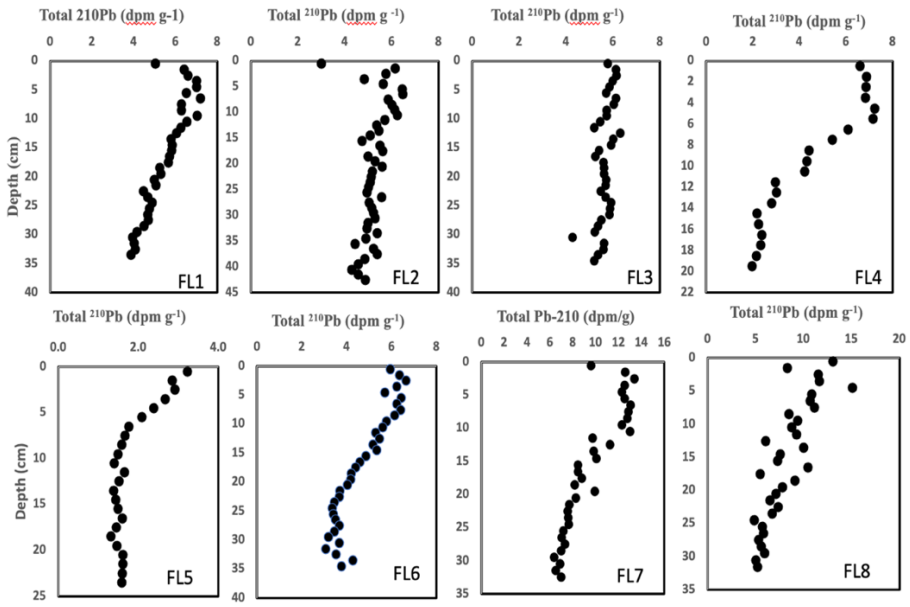

**Figure 8**. Total Pb-210

*Dry Bulk Density and Percent Organic Carbon*

Dry bulk density (DBD) profiles (Appendix Figure 15) display a uniform increase with depth as a function of decreased porosity, ranging from values of 0.2 g $cm^{-3}$ near the surface to 0.7 g $cm^{-3}$ at depth. Percent organic carbon profiles (Appendix Fig. 16) display a range of values from low (less than 2% OC at FL5) to high (7-8% OC at FL7 and FL8). Values for all other cores center around a mean value of approximately 4.5% OC. The % OC values are variable downcore but there is no discernable overall trend towards either increasing or decreasing % OC over the length of the cores.

*Sediment Accumulation Rate and Mass Accumulation Rate*

Based on the outputs of Constant Flux modeling, sediment accumulation rates (SAR) (Figure 9) are relatively constant with depth for all eight cores. Three distinct sedimentation regimes are observed within the reservoir. SAR values increase from FL1 to FL3, followed by a dramatic drop in rates at sites FL 4, 5 and 6 (~30 times lower than FL3). SAR values at FL7 and 8, in the distal portion of the reservoir, exhibit SAR values similar to FL1 and 2. The Mass Accumulation Rates (MAR) for these cores (Appendix Figure 17) follow a similar trend spatially but exhibit less variation with depth than SAR profiles, because MAR accounts for the effects of compaction.

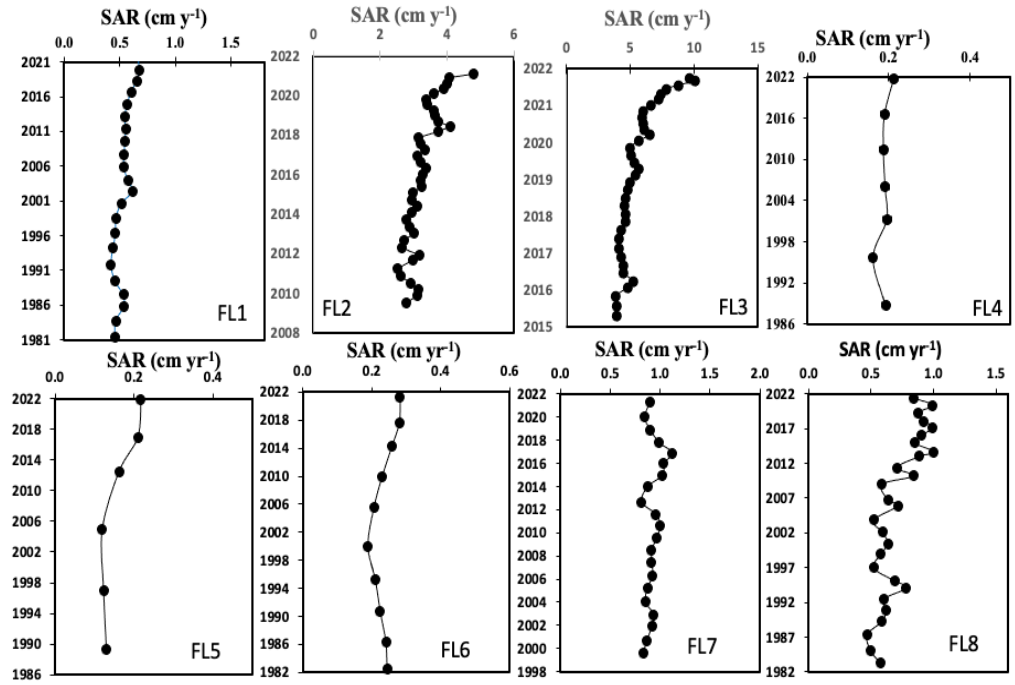


**Figure 9.** Sediment Accumulation Rates (SAR) profile FL1 (cm $y^{-1}$) . Mass Accumulation Rate profiles are displayed in Appendix Figure 17.

*Carbon Accumulation Rate*

The Carbon Accumulation Rate (CAR) profiles (Figure 5) mostly reflect the spatial and depth trends of MAR. Carbon Accumulation Rate (CAR) = MAR * f, where f is the fraction of organic carbon (%C ÷1000). There is significant variation in CAR between individual cores, with the same proximal to distal regime variations as seem in the SAR and MAR plots. FL1, 2, and 3 display high values of CAR, increasing towards FL3, which again is the lake maximum value at 1,752.9 g $C/m^2y$. Sites 4 to 6 exhibit CAR values that are two orders of magnitude lower. The most distal sites, 7 and 8 show a modest recovery in CAR approaching the values of FL1.Though there is certainly some variation in CAR with depth in all cores, the variation is centered around a mean value and there is no significant increasing or decreasing trend with depth. At sites FL1, 2, 3, 7, and 8, $^{210}Pb_{xs}$ inventories were greater than predicted based on calculated atmospheric flux. This indicates that these are sites of sediment focusing. Sites FL4,

5, and 6 have inventory values in the accumulation zone that are less than that supported by atmospheric flux of $^{210}Pb_{xs}$, indicating that at these sites there is an overall loss of deposited sediment over time and that much sediment at these sites is redistributed to other locations.

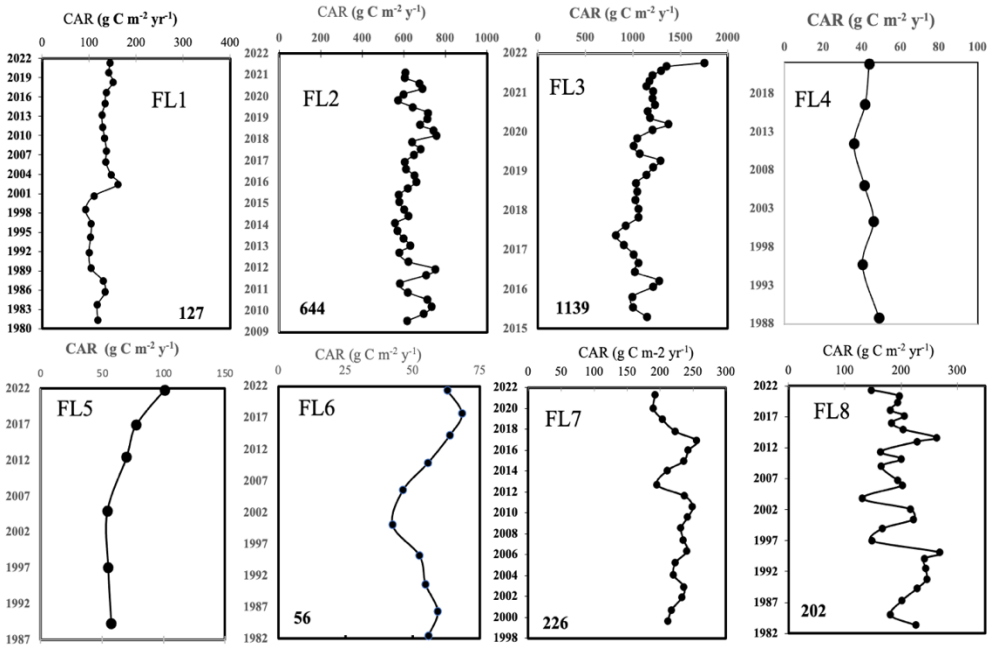


**Figure 10.** Carbon Accumulation Rate (CAR) profile (g C $m^{-2}$ $yr^{-1}$)

Objective 3: Stable Isotopes ($\partial$ $^{15}N$, $\partial$ $^{13}C$) and C:N ratios were used to determine organic carbon sources Previous studies (Kendall et al. 2001, Wang et al. 2020, and Duan et al. 2022) have identified freshwater algae (FWA) source in lakes and reservoirs as having a signal of C:N 7 to 9, $\partial$ $^{13}C$ -32 to -36, and $\partial$ $^{15}N$ 3 to 7. Other publications (Kendall et al. 2001, Findley and Kendall 2007, and Duan et al. 2022) have identified Soil Organic Matter (SOM) as having a signal of C:N 6 to 15, $\partial$ $^{13}C$ -22 to -32, and $\partial$ $^{15}N$ 2 to 6. Figures 11 and 12 displays the Stable Isotopes ($\partial$ $^{15}N$, $\partial$ $^{13}C$) and C:N ratios for water inputs from Ellerbe Creek (EC), Eno River (ER) and Flat River (FR). Only Flat River has a FWA signal. Suspended sediments there had a high organic carbon content. Ellerbe Creek and Eno River has a dominant signal for soild organinc matter.

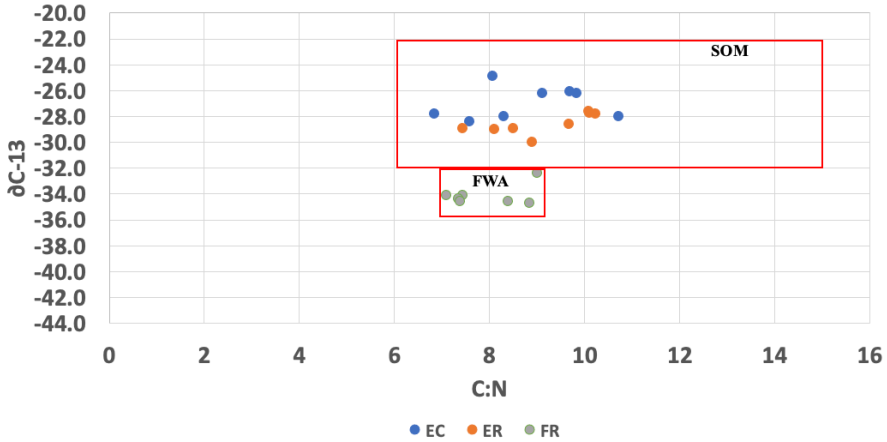


Figure 11. $\partial$ $^{13}C$ vs.C:N ratio for Ellerbe Creek, Eno River and Flat River

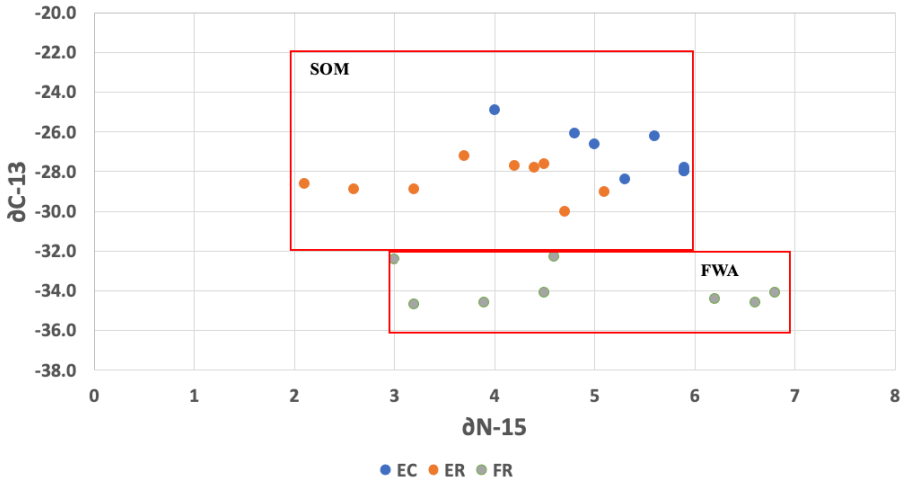


Figure 12 $\partial$ $^{15}$N vs $\partial$ $^{13}$C for for Ellerbe Creek, Eno River and Flat River

When sediments in cores FL1and FL7 are examined, only a signal for soil organinc matter is preserved. This means that either the FWA signal for sediments deposited on the lake bed is minimal or that after deposition the FWA carbon is rapidly decomposed and is not preserved in lake bottom sediments.

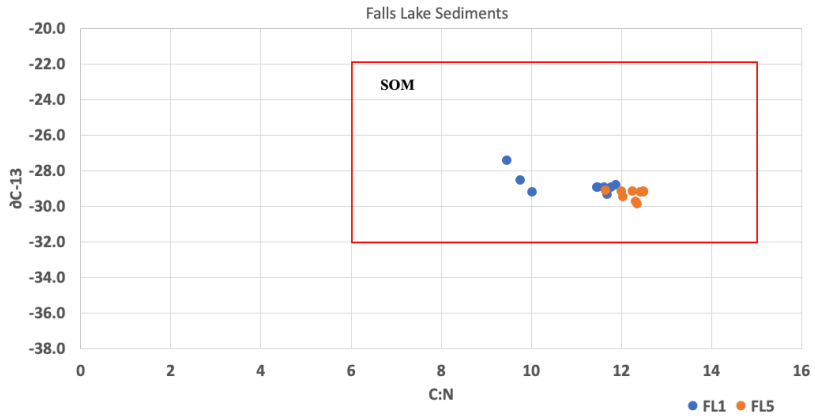


Fig. 13 Figure 13. C:N vs $\partial$ $^{13}$C for core locations FL1 and FL7.

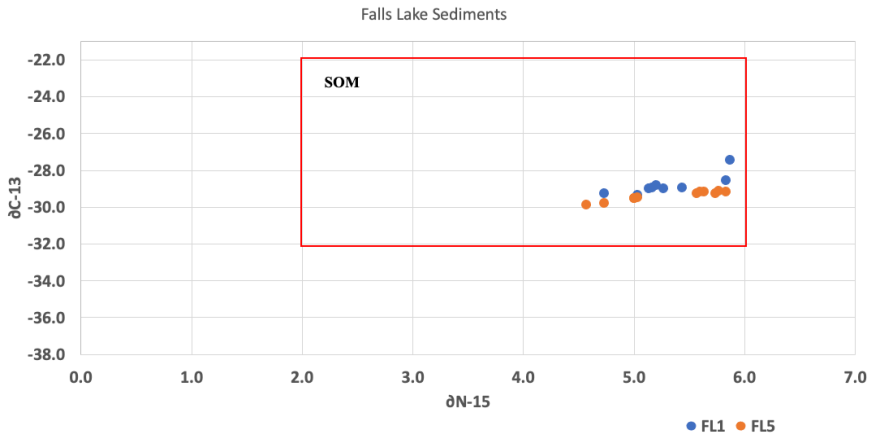


Figure 14. $\partial\ ^{15}N$ vs $\partial\ ^{13}C$ for core locations FL1 and FL7.

C:N, $\partial\ ^{13}C$, and $\partial\ ^{15}N$ worked well to distinguish organic matter sources between river and stream inputs (SOM) and in situ algae production (FWA). Evidence of a FWA source was found in water column samples but only SOM derived carbon sources were detected in Falls Lake Sediments. If other reservoirs are similar in nature to Falls Lake, then the organic carbon accumulating in reservoirs (to offset growing $CO_2$ concentrations in the atmosphere) is primarily from the carbon from reservoir watersheds which are better preserved and stored in reservoir bottom sediments. This conclusion is contrary to the idea that the source of the sedimentary carbon in bottom sediments results from the input of excess nutrients to reservoirs that results in large seasonal algae blooms and low oxygen waters.

**Research Methods**

Question 1: Four rivers and creeks were sampled approximately every two weeks to collect water samples (see "USGS Water Discharge Site Locations"; Appendix Figure 7). The Four input sources examined (Eno River, Flat River, Little River and Ellerbe Creek ) collectively supply approximately 70% of the water and suspended sediments to Falls Lake. Water sampling dates/times were chosen to cover a wide range in water discharge rates observed.

Samples were collected during low, medium and high water-discharge stages so that sediment rating curves represent a wide range of conditions. A sediment rating curve was constructed for each of the 4 water inputs. A separate water sample was collected for POC determination at each of the four sites during each sampling time. We closely monitored water discharge at these four sites and strategically collected samples to completely cover the spectrum of water discharge rates over the course of a year. A sediment rating curve was constructed (plotting suspended sediment concentrations v. water discharge) for each site. The sediment rating curves were used to help predict sediment inputs to Falls Lake.

One to two liters of river/creek water were collected from surface waters and returned to the McKee Lab for subsequent filtration. Triplicate samples were collected at each site for TSM determination. Pre-weighed polycarbonate filters (0.2-micron pore size) were used (under vacuum) to collect the suspended matter from each water samples. Each filtered sample was dried and then reweighed to determine the particulate mass collected. TSM concentrations (mass per water volume collected) were then calculated, using a standard measurement unit of mg/L (milligram per liter). Pre-combusted glass Microfiber Filters (GF/F 0.7-micron pore size) were used to filter the samples for POC determination. Filters were frozen, freeze dried and the transported under cold, dark conditions to the UNC Institute of Marine Sciences where samples were run on a CHN analyzer to determine particulate carbon and nitrogen concentrations on each filter. Samples were collected at/near USGS stations on each river/creek where continuous water discharge measurements are made and reported online (https://m.waterdata.usgs.gov/) for each station.

Water discharge vs TSM concentration rating curves were established for each of the four rivers/creeks. These rating curves will be used in the future to predict TSM concentrations and sediment discharge rates based on USGS water discharge data readily available online. A TSM vs POC concentration relationship was established for each of the four input rivers/creeks. This relationship yielded insight into how the organic carbon fraction of suspended matter varies over time and space. Water discharge vs POC concentration rating curve relationship was also established for each of the four rivers/creeks. These rating curves were used to predict POC concentrations and the particulate organic carbon flux from each river/creek based on USGS water discharge data readily available online. In most rivers and creeks, TSM concentrations increase with increasing water discharge. This relationship is controlled by the supply of particulate matter from the watershed to the river/creek resulting from landscape erosion and transport. The organic carbon fraction of TSM can vary mainly as a function of watershed land use/land cover and water discharge. Understanding the relationship between TSM and POC concentrations provides insight into the watershed processes that control organic carbon inputs to lakes and can also be useful in predicting organic carbon fluxes to lakes.

Question 2: Sediment cores (~50 cm) were collected by boat using a push corer with a one-way valve. Each core was extruded and subsampled at 1 cm intervals for the length of the core. Each interval was weighed, dried and then reweighed to determine dry bulk density. Each interval was analyzed for the $^{210}$Pb (see method below). The naturally occurring radioisotope $^{210}$Pb (22.3 year half life), was used to establish geochronologies and to quantify sediment and carbon accumulation rates. The distribution of $^{210}$Pb with depth in a collected core is determined by the decay rate of $^{210}$Pb, which is known, and the rate of sedimentation, which is determined from the profile. Once a sedimentation model is established, it provides information regrading the rate of sediment accumulation. When paired with organic carbon concentrations, a carbon sediment accumulation profile can also be determined. Cores were collected at 8

locations (Figure 1) distributed from the upper reservoir closest to the major freshwater inputs (FL1) to the lower reservoir closest to the dam (FL8). A push-corer was used to minimize disturbance and cores were transported back in a vertical position, extruded into 1-cm intervals (~10 $cm^3$) and frozen. Individual intervals were then weighed, freeze-dried, and weighed again for calculating porosity. Dry bulk density values were calculated assuming a particle density of 2.5 g $cm^{-3}$. Disaggregated subsamples were used to measure percent organic matter by loss on ignition (LOI; Heiri et al., 2001). Samples were combusted at 450˚C for 4 hours and then weighed again to obtain ignited mass. The LOI (%) was calculated using the equation: [(dry mass-ignited mass)/dry mass] x 100. A subset of samples was also analyzed on a CHN elemental analyzer, and a calibration curve (%OC = 0.503*%LOI - 0.416 ) was used to convert all samples to % OC.

**$^{210}$Pb geochronologies.**

$^{210}$Pb activities were determined via isotope-dilution alpha spectrometry for the isotope $^{210}$Po, that is in secular equilibrium with grandparent $^{210}$Pb. Fine fraction of the sediment was packed into Teflon vessels, 1.5-2.1 g each. Each sample was treated with 1.0ml (~20 dpm) $^{209}$Po tracer diluted in 1M Certified ACS Plus, hydrochloric acid and 15 ml of Certified ACS Plus, 15M nitric acid. The tracer activity has been obtained using certified natural reference standard IAEA-300. The vials were securely closed and undergone microwave digestion in a Microwave Accelerated Reaction System (MARS 5) for 4 hours and 20 minutes in 3 cycles at temperatures up to 90°C. Cooled vessels were placed under a fume hood. Content of the vessels was transferred to appropriately labeled 50 ml centrifuge tubes. Teflon vessels were rinsed with deionized water to recover all content using minimal amount of DI water- to minimize the sample volume in next steps. Samples were centrifuge at 3500 rpm for 8 minutes in a Thermofisher centrifuge. The separated supernate was transferred into appropriately labeled Teflon beakers and placed on the hotplate. Sediment in each vial was treated with 5ml of 15M nitric acid, vortexed and once more centrifuged at 3500 rpm for 8 minutes. The supernate was combined with the rest of the leached samples in the Teflon beakers on the hot plate. The remaining sediment was discarded. Temperature of the hot plate has been kept between 85-90°C not to exceed 95°C to avoid losses due to volatilization of the $^{209}$Po tracer. When the solution in the beakers has warmed up, 1-2ml of 10.3M hydrogen peroxide was titrated to each beaker and let effervesce. Addition of hydrogen peroxide further degrades organic components not destroyed by heating with nitric acid. Nearly dried samples were then dissolved in 15ml deionized water. In the next step samples were titrated with ammonium hydroxide to raise the pH to 7 – 8.5. Change in pH allowed iron precipitation. Precipitated iron was collected via centrifugation 8 minutes at 3500 rpm and then rinsed twice with 30ml of deionized water. Iron precipitate was dissolved with 3.75ml 10M Certified ACS Plus hydrochloric acid and treated with ~50/60 mg of ascorbic acid to eliminate the interference of iron by reducing it to the ferrous state Fe3+ to Fe2+. Samples were transferred back to Teflon beakers with labeled stainless-steel disks and stirrers. The stainless-steel discs are coated with foil on one side. To assure maximum yields samples were allowed spontaneous deposition for 20-24h with stirrers at 200-300 rpm at room temperature. The next day the discs were removed from a solution, rinsed with a deionized water, and left to air-dry for 24 hours. Planchetes were transferred to α-particle spectrometry utilizing Passivated Implanted Planar Silicon (PIPS®) detector for counting for 24 hours.

Geochronologies were determined using $^{210}$Pb ($t_{1/2}$ = 22.23 yrs), a naturally occurring radionuclide. The fine-grained fraction (<63 microns) for each core interval was analyzed for $^{210}$Pb by isotope-dilution alpha spectrometry. This method assumes that $^{210}$Po, the granddaughter isotope of $^{210}$Pb, is in secular equilibrium with $^{210}$Pb (Flynn, 1968; El-Daoushy et al., 1991; Matthews et al., 2007). Total $^{210}$Pb activity is the sum of the $^{210}$Pb within particle matrices (referred to as a supported) and the $^{210}$Pb sorbed onto particle surfaces (referred to as excess; $^{210}Pb_{xs}$) (DeMaster et al., 1985; Appleby and Oldfield, 1992). Supported levels of $^{210}$Pb ($^{226}$Ra activity) were determined by gamma spectrometry. Sediment samples were freeze-dried, packed into standardized petri dishes, and sealed for three weeks to allow $^{222}$Rn equilibration. Gamma counting was conducted on low-background, high-efficiency germanium detectors

coupled with a multi-channel analyzer. $^{226}$Ra activities were determined by measuring $^{214}$Bi (609 keV). Total $^{210}$Pb activities and dry bulk density, both of which are needed for geochronology modeling, are presented in Supplement Figures S1 and S2. Accumulation rates were determined using a constant flux (CF) model, described in Sanchez-Cabeza and Ruiz-Fernandez (2012). The CF model was used because it allows for variable rates of sedimentation and provides ages and accumulation rates for each discrete interval within the core (Appleby and Oldfield 1978). Depth-integrated inventories of $^{210}Pb_{xs}$ were calculated by summing the product of $^{210}Pb_{xs}$ activity (dpm/g) and dry mass (g/cm$^2$) for all core sections. The complete $^{210}Pb_{xs}$ inventory for each core was used to calculate the $^{210}$Pb flux (inventory multiplied by the decay coefficient for $^{210}$Pb). Expected inventories from atmospheric sources of $^{210}Pb_{xs}$ in North Carolina, based on soil cores (Graustein and Turekian, 1986) and salt-marsh cores (Benninger and Wells, 1993) are ~28 dpm cm$^{-2}$. The $^{210}Pb_{xs}$ atmospheric flux needed to maintain this inventory was calculated to be 0.86 dpm cm$^{-2}$ yr$^{-1}$.

**C/N Concentrations**. Samples for particulate carbon and nitrogen were frozen, freeze dried and transported under cold, dark conditions to the UNC Institute of Marine Sciences where samples were run on a CHN analyzer to determine particulate carbon and nitrogen concentrations. The first is a plot of sediment accumulation rate as a function of depth in the core. This displays the changes in sedimentation rate over the past ~60 year (since Falls Lake reservoir was established). This approach also yields a time history within the sediments of Falls Lake. A set of established time horizons within each core using this method is useful to examine other inputs to Falls Lake over time (e.g., contaminant and nutrient inputs). By pairing the organic carbon concentration in each interval with the age versus depth profile established by $^{210}$Pb, a third product (organic carbon accumulation) is derived.

**$^{210}$Pb Profiles**

Excess $^{210}$Pb profiles for each core, plotted against depth, are shown in Figure 2. All cores, except for FL2 and 3, reached background levels of supported $^{210}$Pb within the core collected and $^{210}Pb_{xs}$ values were calculated as total $^{210}$Pb minus background. The missing $^{210}$Pb inventories and $^{210}Pb_{xs}$ values for FL2 and 3 were calculated based on methods outlined in Appleby (1998). Excess $^{210}$Pb inventories (dpm cm$^{-2}$) for each 1 cm layer is the product of $C_x * DBD_x * X$, where $C_x$ is the $^{210}Pb_{xs}$ activity, $DBD_x$ is the dry bulk density and X is the layer thickness. Surface $^{210}Pb_{xs}$ activities for cores FL1- 4 are similar at ~4 dpm g$^{-1}$, values for FL5 and 6 are much lower (~2 dpm g$^{-1}$), and surface $^{210}Pb_{xs}$ activities for distal sites (FL7 and 8) are highest (~10 dpm g$^{-1}$).

*Dry Bulk Density and Percent Organic Carbon*

Dry bulk density (DBD) profiles (Supplement Figure S2) display a uniform increase with depth as a function of decreased porosity, ranging from values of 0.2 g cm$^{-3}$ near the surface to 0.7 g cm$^{-3}$ at depth. Percent organic carbon profiles (Figure 3) display a range of values from low (less than 2% OC at FL5) to high (7-8% OC at FL7 and FL8). Values for all other cores center around a mean value of approximately 4.5% OC. The % OC values are variable downcore but there is no discernable overall trend towards either increasing or decreasing % OC over the length of the cores.

***Sediment and Carbon Accumulation Rates***

Based on the outputs of CF modeling, sediment accumulation rates (SAR) (Figure 4) are relatively constant with depth for all eight cores. Three distinct sedimentation regimes are observed within the reservoir. SAR values increase from FL1 to FL3, followed by a dramatic drop in rates at sites FL 4, 5 and 6 (~30 times lower than FL3). SAR values at FL7 and 8, in the distal portion of the reservoir, exhibit SAR values similar to FL1 and 2. The Mass Accumulation Rates (MAR) for these cores (Supplement Figure S3) follow a similar trend spatially but exhibit less variation with depth than SAR profiles, because MAR accounts for the effects of compaction.

The Carbon Accumulation Rate (CAR) profiles (Figure 5) mostly reflect the spatial and depth trends of MAR. Carbon Accumulation Rate (CAR) = MAR * f, where f is the fraction of organic carbon (%C ÷1000). There is significant variation in CAR between individual cores, with the same proximal to distal regime variations as seem in the SAR and MAR plots. FL1, 2, and 3 display high values of CAR, increasing towards FL3, which again is the lake maximum value at 1,752.9 g C/$m^2$y. Sites 4 to 6 exhibit CAR values that are two orders of magnitude lower. The most distal sites, 7 and 8 show a modest recovery in CAR approaching the values of FL1.Though there is certainly some variation in CAR with depth in all cores, the variation is centered around a mean value and there is no significant increasing or decreasing trend with depth. At sites FL1, 2, 3, 7, and 8, $^{210}Pb_{xs}$ inventories were greater than predicted based on calculated atmospheric flux. This indicates that these are sites of sediment focusing. Sites FL4, 5, and 6 have inventory values in the accumulation zone that are less than that supported by atmospheric flux of $^{210}Pb_{xs}$, indicating that at these sites there is an overall loss of deposited sediment over time and that much sediment at these sites is redistributed to other locations.

Objective 3: Stable Isotope determinization ($^{15}N$ and $^{13}C$). Previous publications (*Kendall et al. 2001*, *Wang et al. 2020*, and *Duan et al. 2022*) have defined Fresh Water Algal (FWA) signal as :C:N 7 to 9, $\partial\ ^{13}C$ -32 to -36, and $\partial\ ^{15}N$ 3 to 7. Other pubications (*Kendall et al. 2001*, *Findley and Kendall 2007*, and *Duan et al. 2022*)have defined Soil Organc Matter (SOM) signal as C:N 6 to 15, $\partial\ ^{13}C$ -22 to -32, $\partial\ ^{15}N$ 2 to 6. Using those definitions, we group FWA and SOM for Ellerbe Creek (EC), Eno River (ER) and Flat River (FL).

# Management Implications and Recommendations

The results of this study can be used to answer a few overall questions about carbon accumulation in this reservoir that have management implications:

*(a) What drives carbon accumulation?*

Many possible factors are potential drivers of carbon accumulation within an aquatic system. The major drivers may vary significantly based on the ecosystem studied. Based on the factors used to calculate carbon accumulation, CAR is the product of MAR * f, where f is the fraction of organic carbon (%C ÷1000). Therefore, the two potential major drivers for carbon accumulation in must be either sediment accumulation rate or organic carbon content. All CAR values are plotted against %OC and MAR in Figure 15, which shows a very strong correlation between CAR and MAR ($R^2$= .9905) and no discernable correlation between CAR and %OC. This suggests MAR is a very strong control on CAR within Falls Lake, likely because of the dominance of an allochthonous source of material from the watershed.

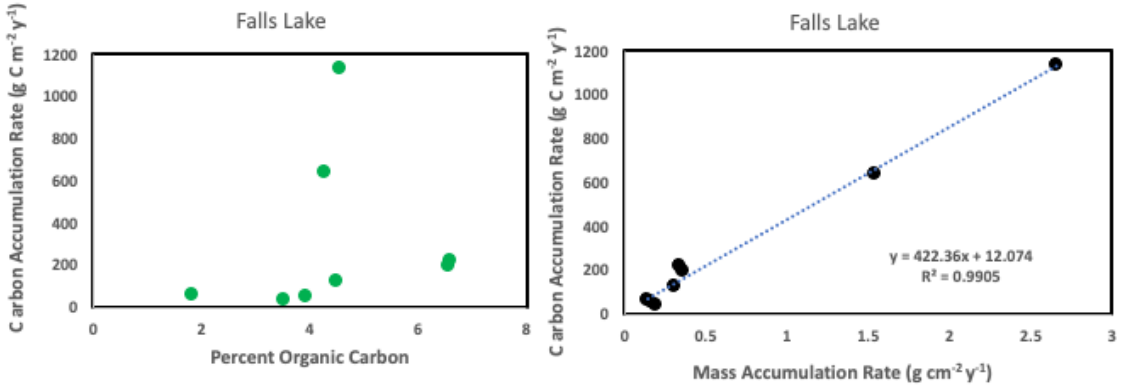


**Figure 15**. Carbon Accumulation Rate vs. %OC and MAR (cores FL1 – FL8).

(b) *Have CARs changed over the past 40 years?*

Downcore profiles within Falls Lake indicate that CAR has not changed significantly since the reservoir's construction in the early 1980s (Figure 10). No core shows a significant, progressive increase that would be consistent with a response to rising atmospheric carbon concentrations, nor do they show a significant basin-wide trend. These trends are consistent with the idea that MAR controls CAR. Because SAR and MAR have remained relatively constant over time throughout Falls Lake, we can also assume watershed inputs have not varied greatly since the reservoir's creation. However, this steady input may potential vary in the future with regional land use changes as the area continues to be a hub of human development. Ongoing deforestation and rises in stormwater runoff resulting from urbanization could result in increasing erosion within the watershed and provide more allochthonous materials to be potentially stored within the reservoir.

(c) *How do reservoirs compare to other significant carbon depocenters such as Blue Carbon environments (marshes, mangroves, seagrass), natural lakes, and estuaries?*

Blue carbon environments have recently been recognized as ecosystems that are high in carbon sequestration and therefore have received significant attention that has resulted in numerous publications in recent years (Bulmer et al. 2020). Similarly, natural lakes and estuaries have also been studied

extensively for their carbon sequestration potential. Manmade reservoirs have not experienced the same level of attention and have largely been underappreciated as terrestrial carbon sinks. The results of our study indicate Falls Lake is comparable and, in some cases, may exceed the CARs of many of these high carbon burial ecosystems, which range in mean values from 138 g C $m^{-2}y^{-1}$ for seagrass beds to 226 g C $m^{-2}y^{-1}$ for mangroves (Table 4). The mean CAR of cores collected in Lake range from 43 to 1139 g C $m^{-2}y^{-1}$, with a mean value of 313 g C $m^{-2}y^{-1}$, on par with the reported CAR values for various blue carbon environments. The indication is that reservoirs are comparable as carbon sinks to ecosystems that have received significantly more attention. Falls Lake shows higher CARs even in the areas of lowest accumulation than recent values for global lake carbon accumulation, which have a mean of 22 g C $m^{-2}y^{-1}$ (Mendonça et al. 2017, n = 344). This suggests that the unique dynamics of reservoirs compared to outwardly similar natural lakes makes them much more accommodating for sediment and carbon burial (Hayes et al., 2017). The potential of reservoirs showcased by Falls Lake, combined with the dramatically increasing prevalence of reservoirs globally, demonstrate the growing need for more quantitative, rigorous, and repeatable data to rigorously quantify reservoirs as major terrestrial carbon sinks.

Table 1: Carbon burial in Falls Lake compared to other depositional environments

| **Ecosystem** | **Carbon "burial" rate (g C $m^{-2}$ $y^{-1}$)** | **Source** |
|---|---|---|
| Salt Marshes | **218**<br>(range = 18 – 1713)<br>n = 96 sites | McLeod et al. 2011 |
| Mangroves | **226**<br>(range = 20-949)<br>n = 34 sites | McLeod et al. 2011 |
| Seagrasses | **138**<br>(range = 45 -190)<br>n = 123 sites | McLeod et al. 2011 |
| Falls Lake Reservoir | **313**<br>(range = 42 – 1139)<br>n = 8 | This study |

8.

**Researchers, university affiliation, and department**

Brent McKee, Sherif Ghobrial, Scott Booth, and Alyson Burch
Department of Earth, Marine and Environmental Sciences
University of North Carolina at Chapel Hill

APPENDIX: McKee

## Site Information
## USGS Water Discharge Site Locations

**Appendix Table 1**

Site Number: 02086849
Site Name: **ELLERBE CREEK NEAR GORMAN, NC**
Site Type: Stream
Agency: USGS
Latitude 36°03'33" N 78°49'58" W NAD27
Durham County, North Carolina, Hydrologic Unit 03020201
Drainage area: 21.9 square miles
Datum of gage: 252.31 feet above NAVD88.

Site Number: 02086500
Site Name: **FLAT RIVER AT DAM NEAR BAHAMA, NC**
Site Type: Stream
Agency: USGS
Latitude 36°08'55" N 78°49'44" W NAD83
Durham County, North Carolina, Hydrologic Unit 03020201
Drainage area: 168 square miles
Datum of gage: 256.60 feet above NGVD29.

Site Number: 0208524975
Site Name: **LITTLE R BL LITTLE R TRIB AT FAIRNTOSH, NC**
Site Type: Stream
Agency: USGS
Latitude 36°06'48" N. 78°51'35" W NAD83
Durham County, North Carolina, Hydrologic Unit 03020201
Drainage area: 98.9 square miles
Datum of gage: 263.6 feet above NAVD88

Site Number: 02085070
Site Name: **ENO RIVER NEAR DURHAM, NC**
Site Type: Stream
Agency: USGS
Latitude 36°04'20" N 78°54'28" W NAD83
Durham County, North Carolina, Hydrologic Unit 03020201
Drainage area: 141 square miles
Datum of gage: 269.92 feet above NAVD88

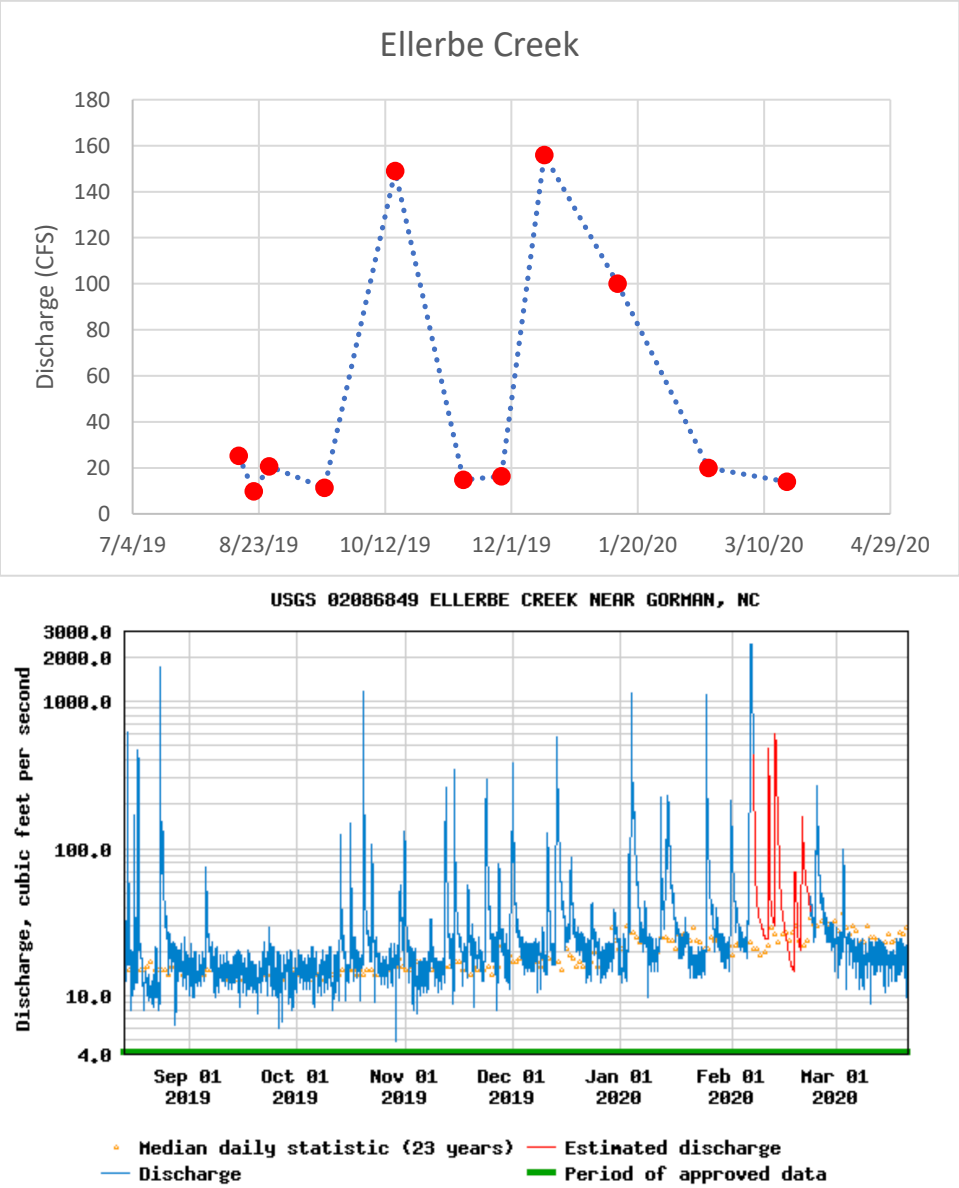


**Figure 1** shows the relationship between discharge (cubic feet per second; CFS) and the dates the eleven (11) samples collected for Ellerbe Creek. Discharge for Ellerbe Creek (near Gorman) remained steady across eight of the eleven sampling dates and showed a significant increase in discharge for 10/16/ 19, 12/14/19 and 1/12/20.

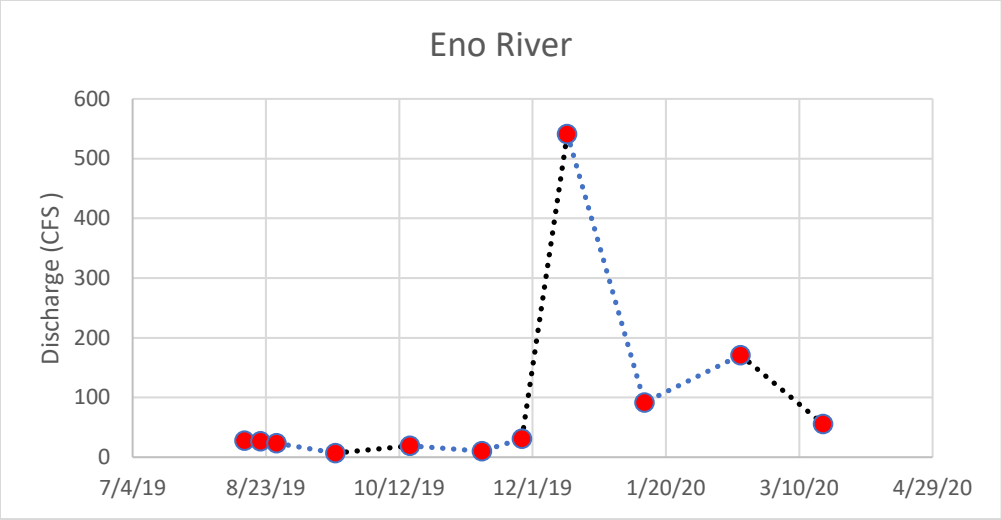


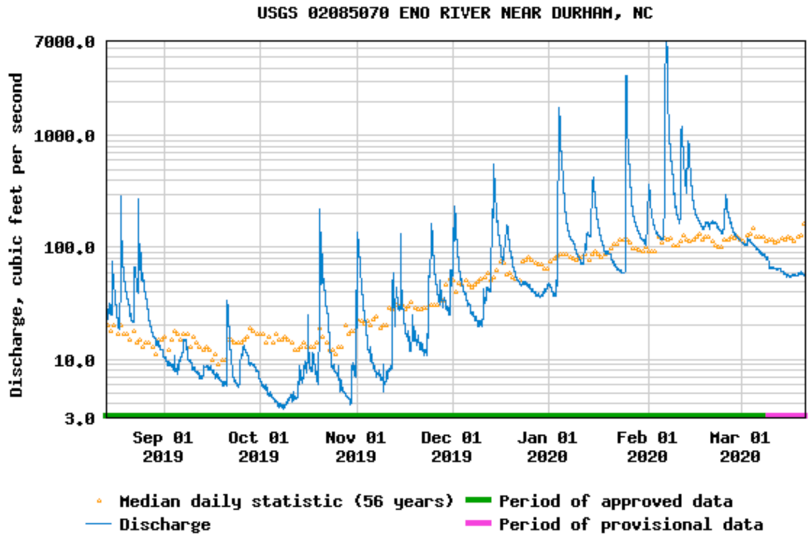


**Figure 2** Shows the relationship between discharge and the dates the samples were collected for Eno River.

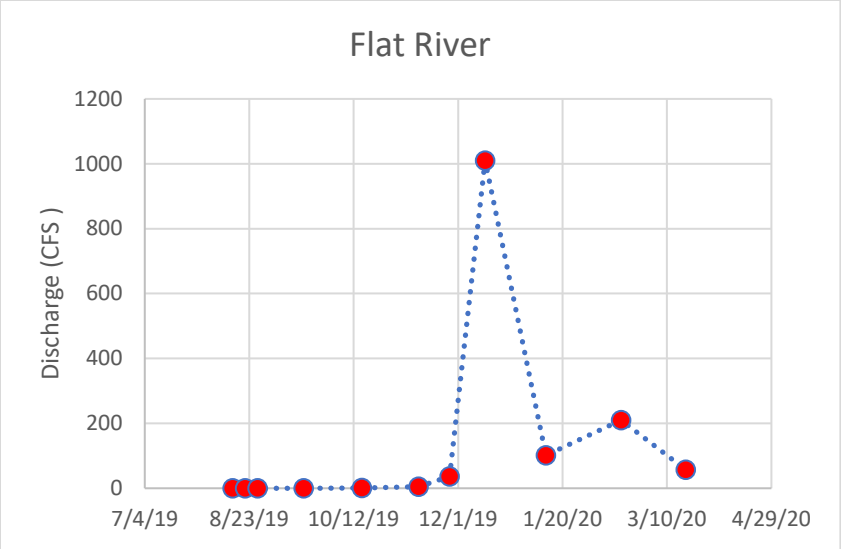


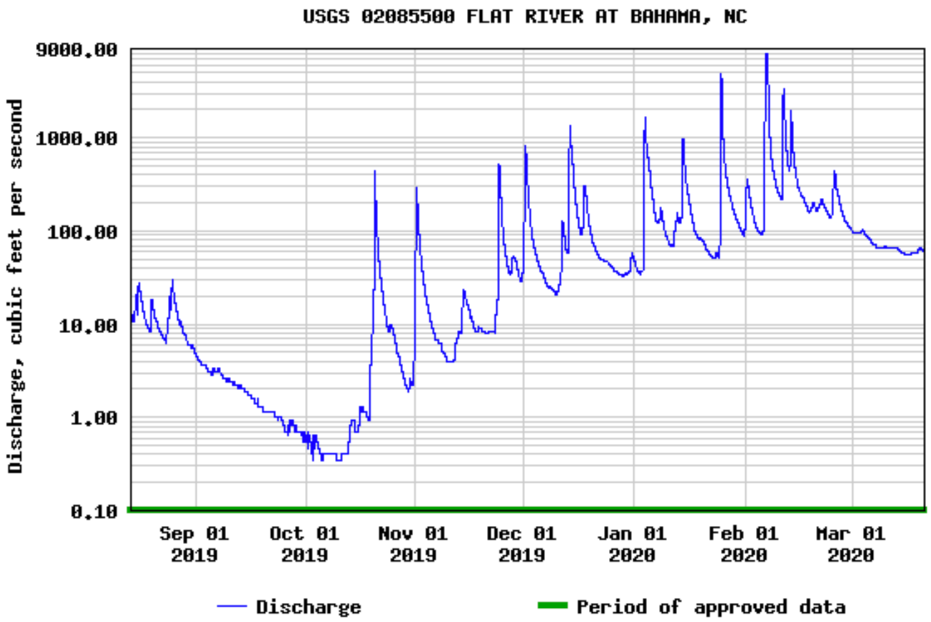


**Figure 3** Shows the relationship between discharge and the date the samples were collected for Flat River.

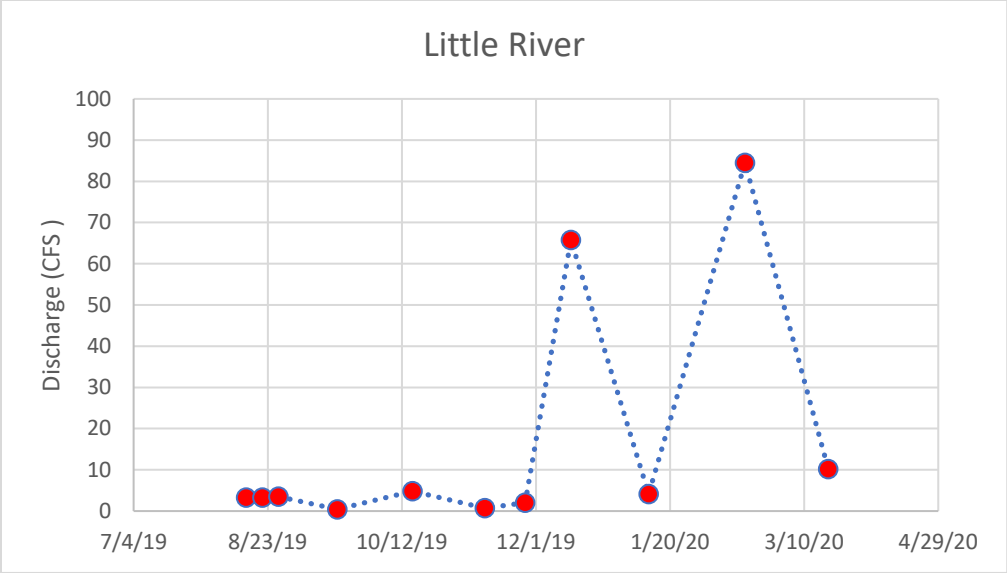


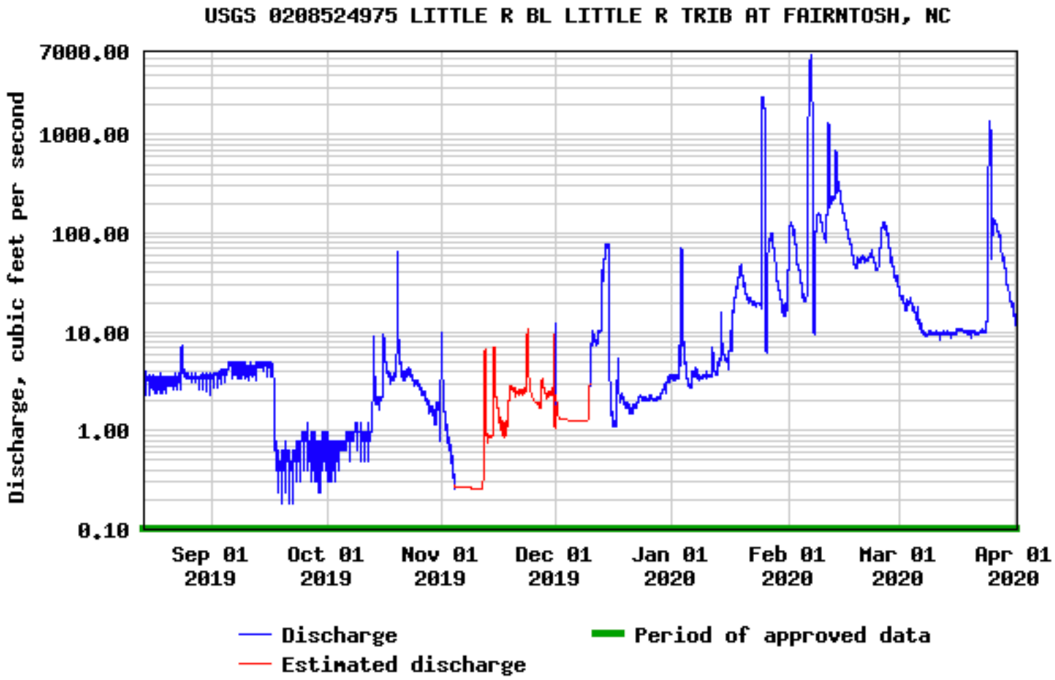


**Figure 4** Shows the relationship between discharge and the date the samples were collected for Little River.

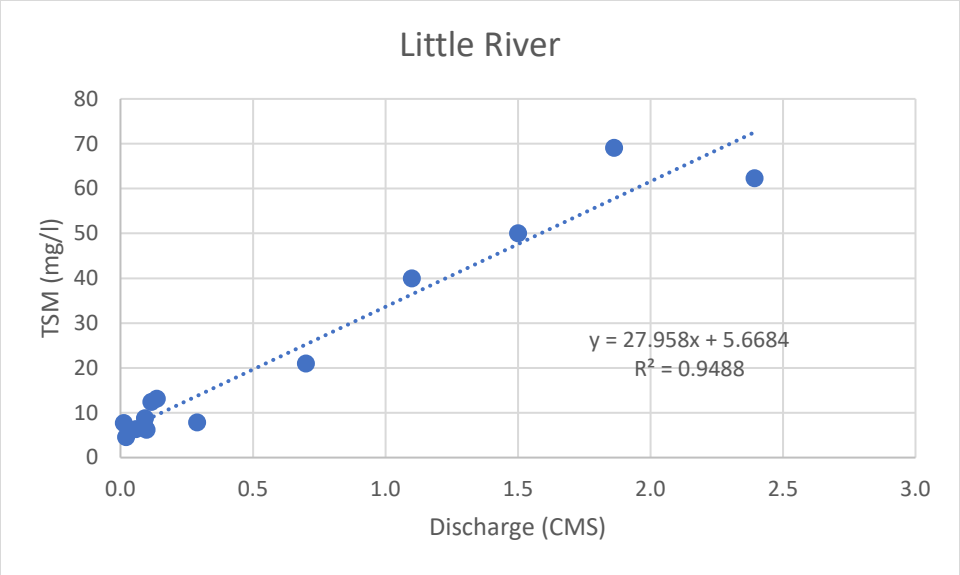


**Figure 4** shows the relationship between water discharge (CMS cubic meters per second) and TSM (total suspended matter; mg/l) for Little River

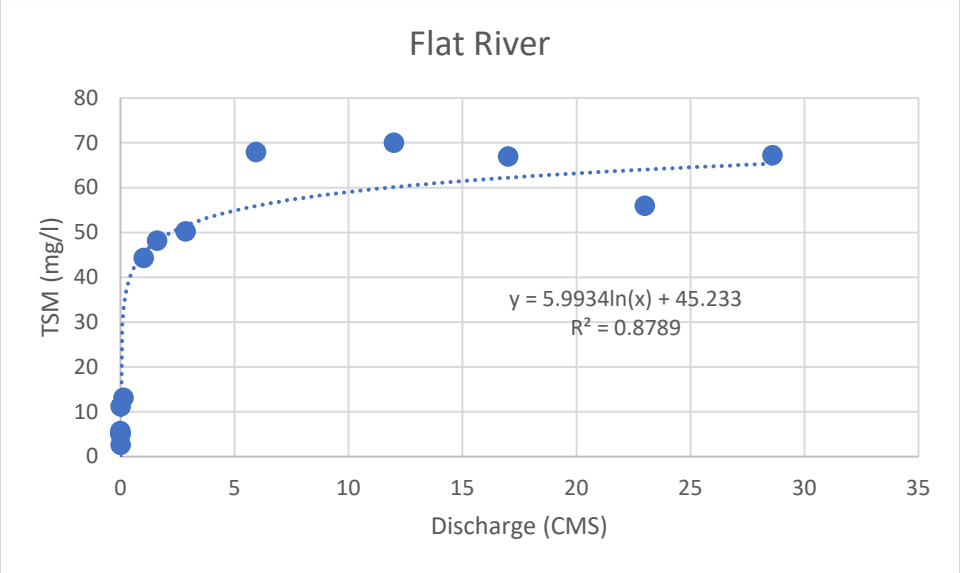


**Figure 5.** shows the relationship between water discharge (CMS cubic meters per second) and TSM (total suspended matter; mg/l) for Flat River

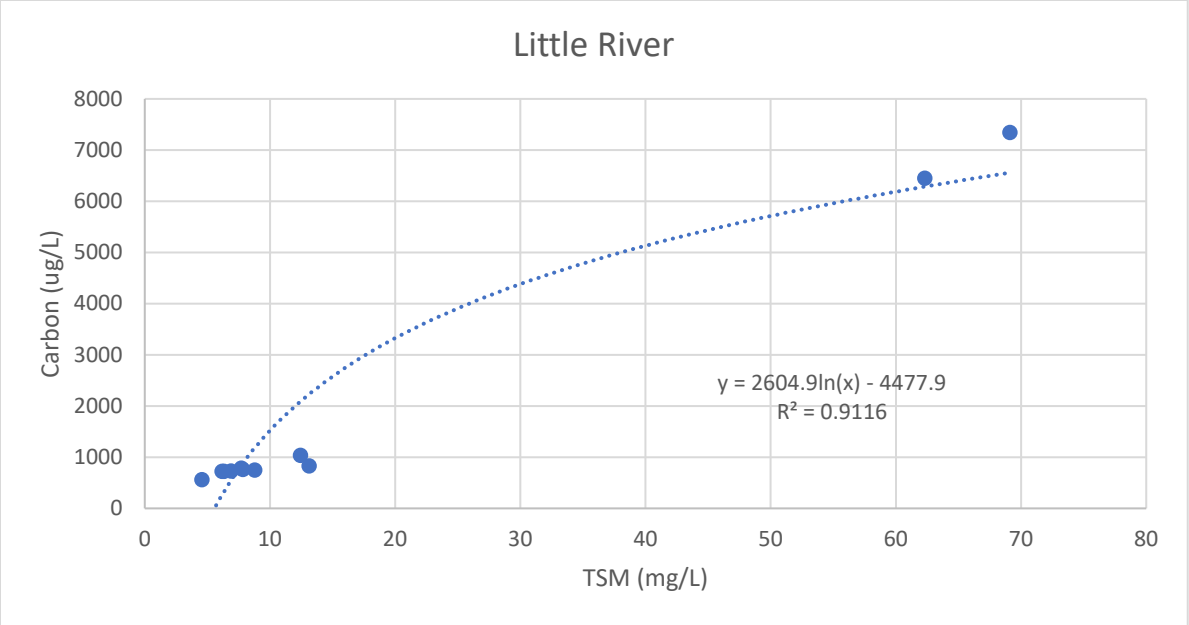


**Figure 6** Shows the relationship between TSM and carbon (ug/L) for the Little River.

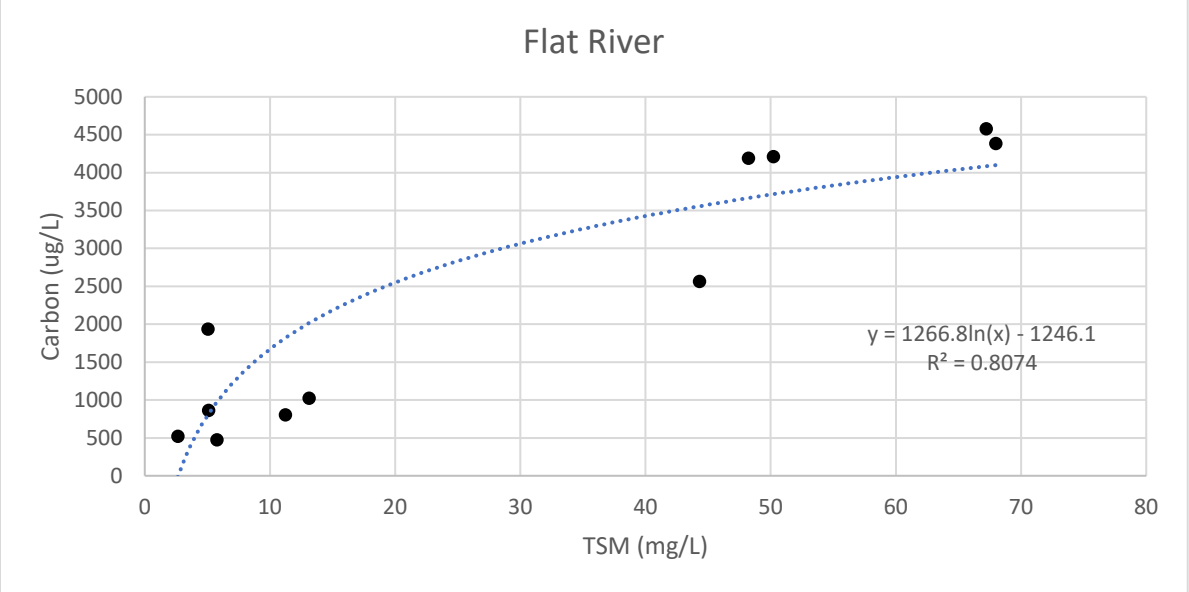


**Figure 7** Shows the relationship between TSM and carbon (ug/L) for the Flat River.

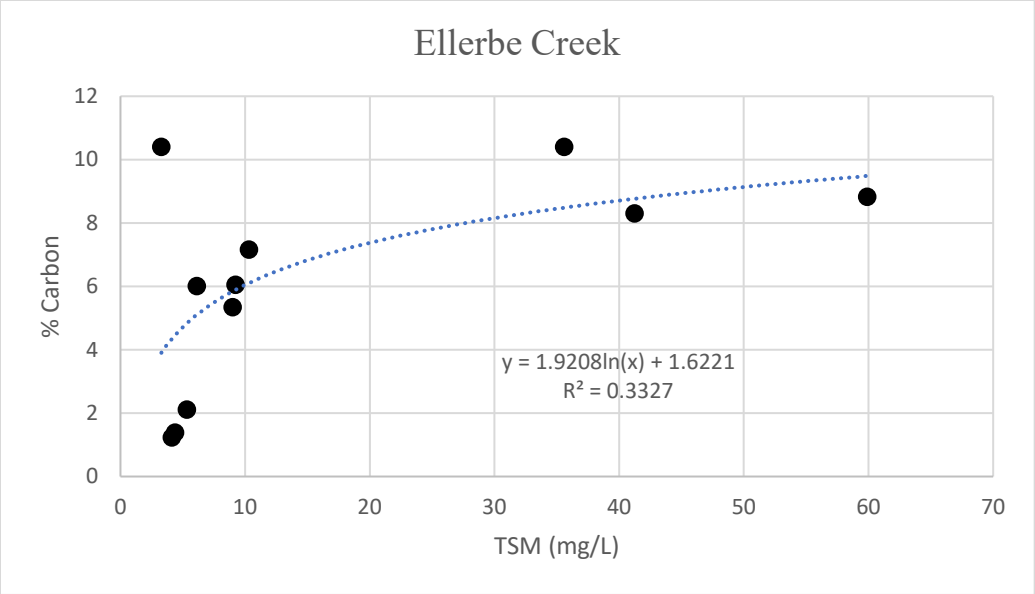


**Figure 8** Shows the relationship between TSM and % carbon for Ellerbe Creek

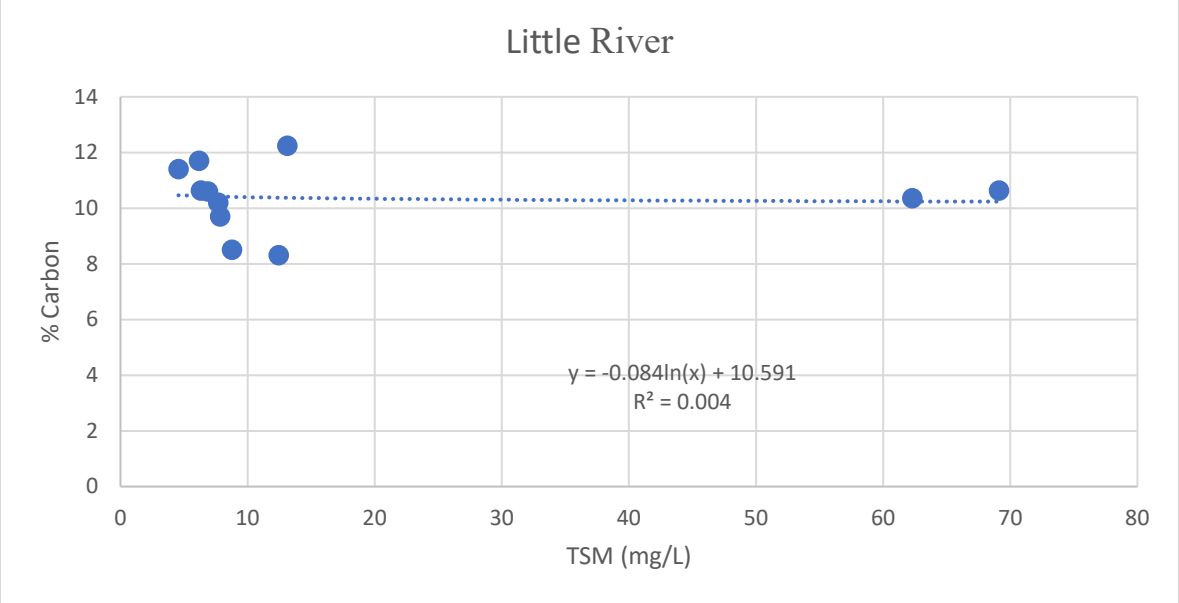


**Figure 9.** Shows the relationship between TSM and % carbon for the Little River.

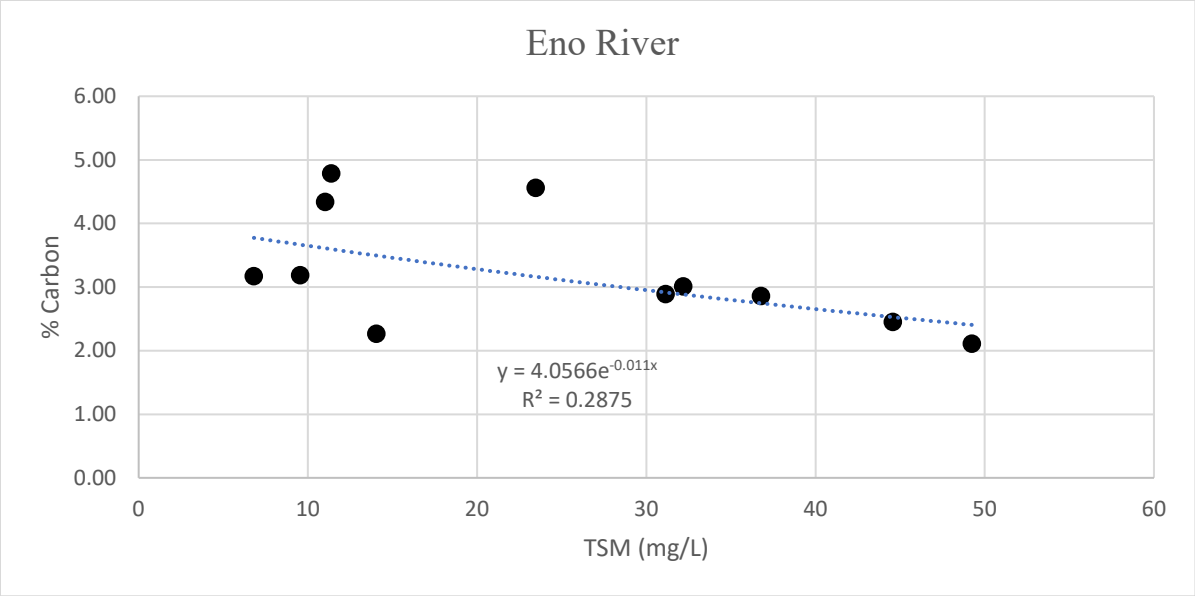


**Figure 10.** Shows the relationship between TSM and % carbon for the Eno River.

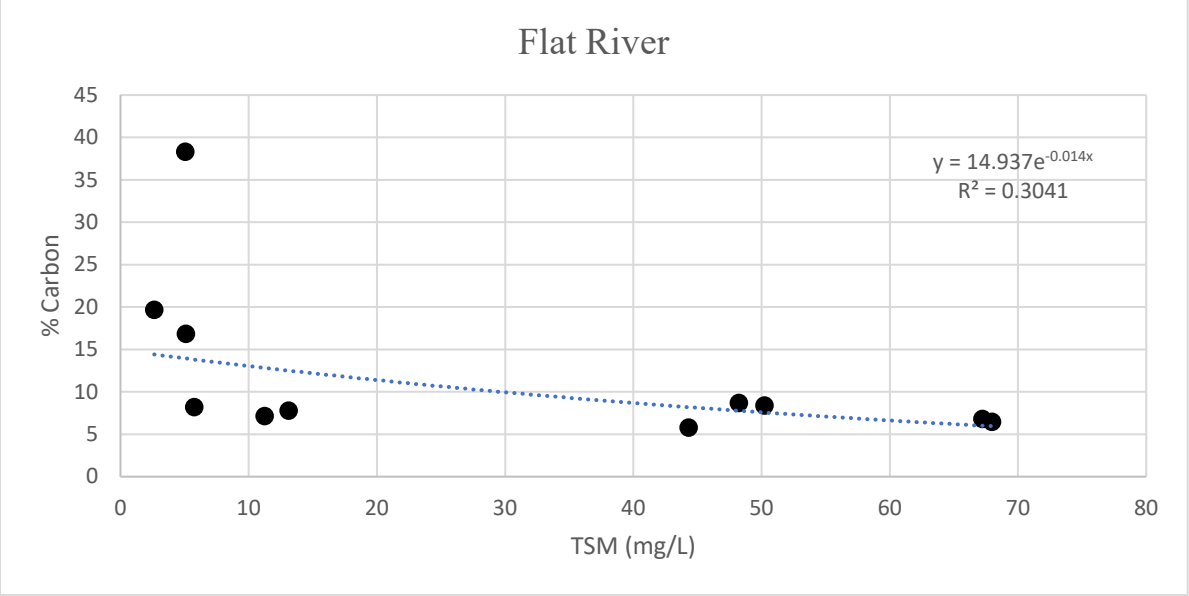


**Figure 11.** Shows the relationship between TSM and % carbon for the Flat River

The correlation between C:N ratio and TSM is poor for Eno, Flat and Little Rivers (Appendix Fig. 12 - 14) indicating that the organic carbon is similar within these watershed.

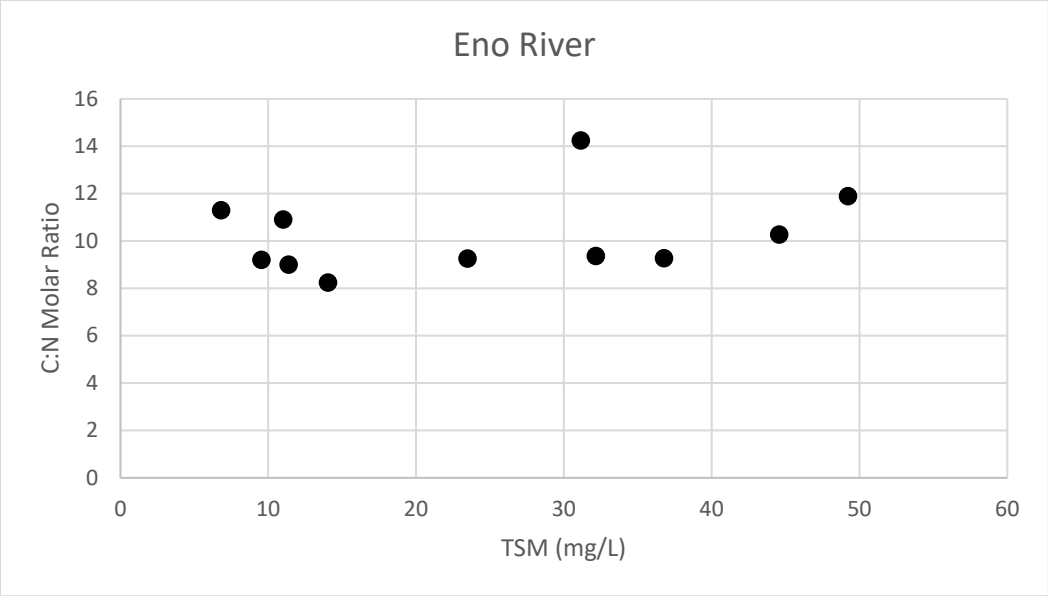


**Figure 12** Shows the relationship between the C:N ratio and discharge for Eno River. Mean value is 10.27

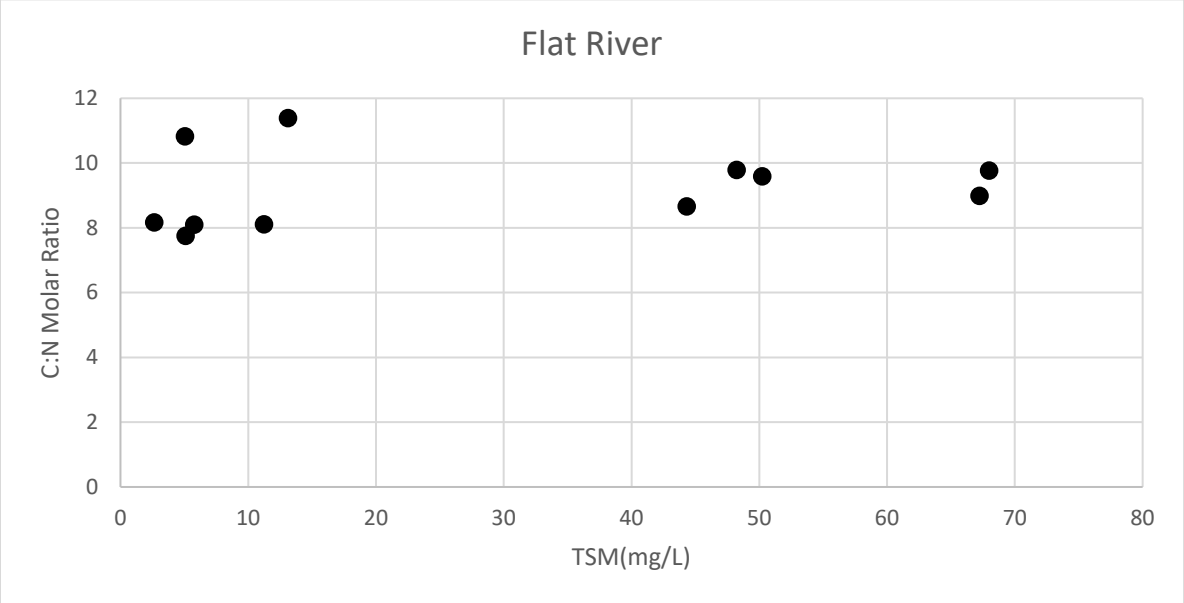


**Figure 13** Shows the relationship between the C:N ratio and discharge for Flat River. Mean value is 9.19

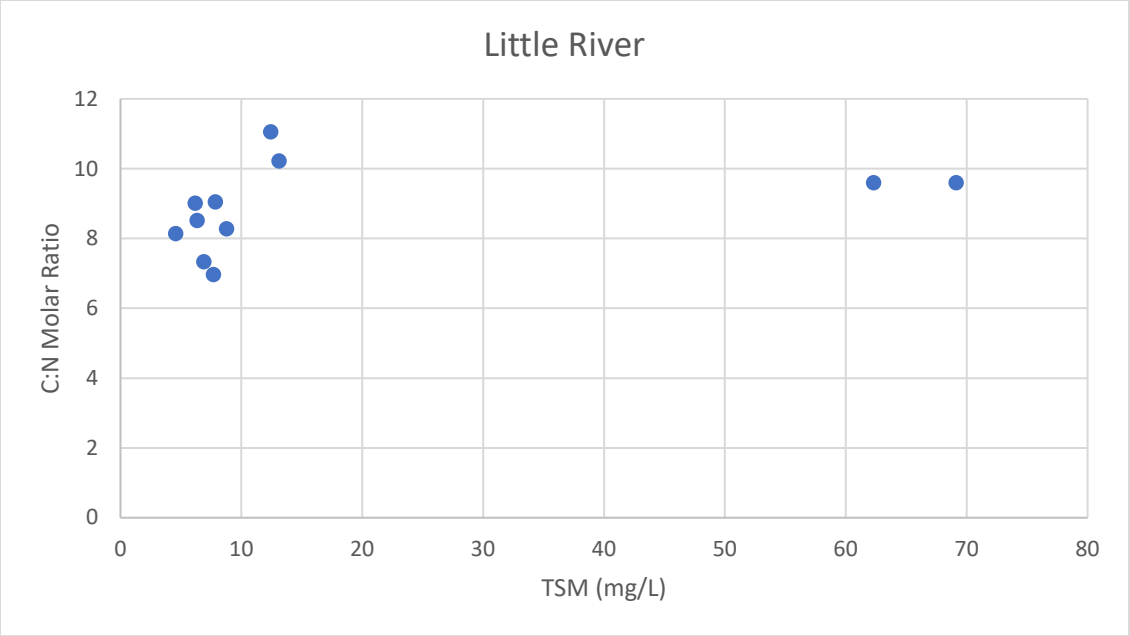


**Figure 14** Shows the relationship between the C:N ratio and discharge for Little River. Mean values is 8.89

Table 2: Location Information for Coring location

| Station | Date Collected | Location | Core Length |
|---|---|---|---|
| FL1 | 03/25/2021 | 36.051066°N 78.761890°W | 41 |
| FL2 | 10/23/2021 | 36.030664°N 78.758037°W | 43 |
| FL3 | 10/23/2021 | 36.017483°N 78.735633°W | 41 |
| FL4 | 10/23/2021 | 36.027821°N 78.728694°W | 20 |
| FL5 | 10/23/2021 | 36.030217°N 78.715017°W | 24 |
| FL6 | 04/26/2021 | 36.017189°N 78.720879°W | 35 |
| FL7 | 04/12/2021 | 36.002228°N 78.652618°W | 36 |
| FL8 | 04/26/2021 | 36.954434°N 78.580062°W | 33 |

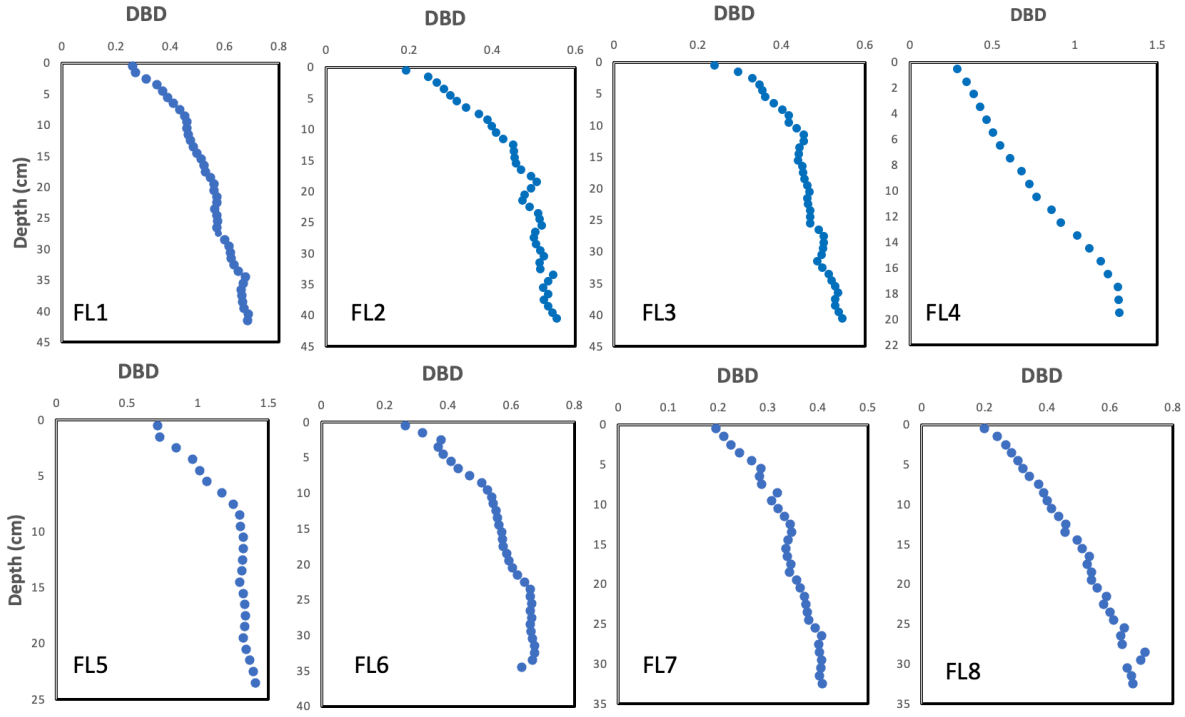


**Appendix Figure 15.** Dry Bulk Density (DBD)

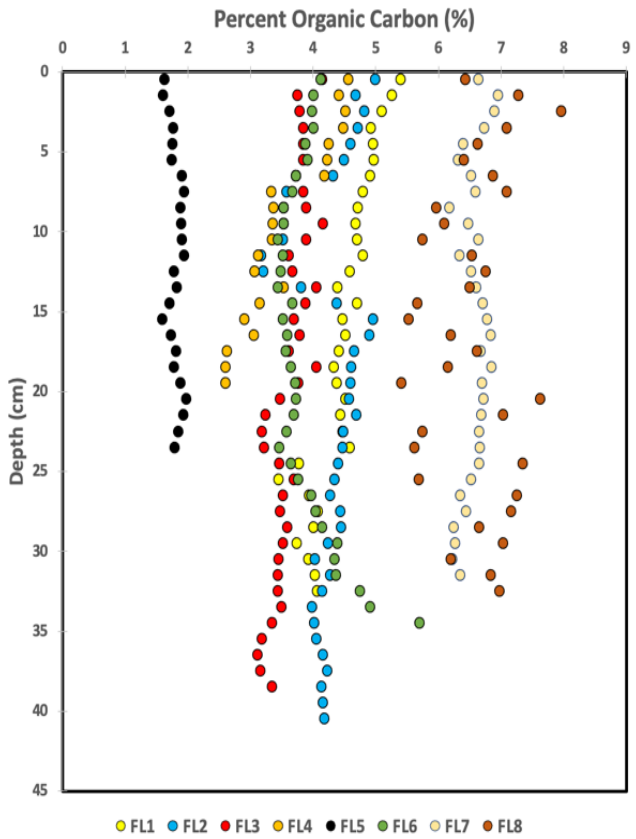


**Appendix Fig. 16.** Percent Organic Carbon profiles for cores 1 through

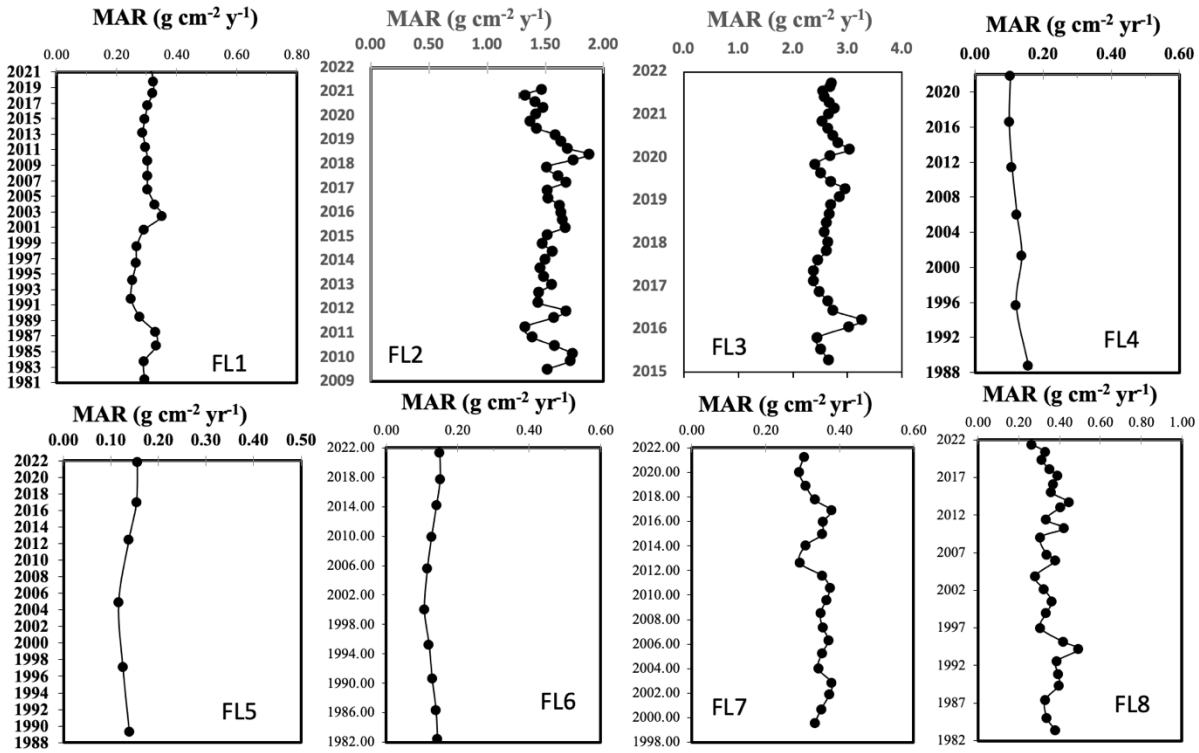


**Appendix Figure 17**. Mass Accumulation Rates (MAR)